### Study Limitations

This study has the following limitations: (1) a small sample size, which is inadequate for statistical analysis; (2) transplantation of TCD-51073 occurred in the absence of other concomitant therapies, so an add-on effect is unlikely to occur in the before-and-after comparisons; however, comparison with a group of untreated patients is necessary; (3) single-arm, open-label study, so the possibility of assessment bias cannot be ruled out; an independent analysis should be considered; and (4) the evaluation period of 26 weeks after transplantation is limited for demonstrating the efficacy of TCD-51073 in improving survival outcomes and preventing hospitalizations because of HF, thus requiring further mid- and long-term follow-up data.

## Conclusions

This study demonstrated the feasibility and safety of the transplantation of TCD-51073 in patients with severe chronic HF due to ischemic heart disease, suggesting that TCD-51073 might maintain or improve cardiac function, symptoms, and physical function.

### Acknowledgments

We thank all of the investigators and site staff who participated in this clinical study.

### Disclosures

UMIN study Identifier: UMIN000008013. Sponsor/Name of Grant: Terumo Corporation.

All authors serve as investigators in this trial. Y. Sawa has received joint research funds provided by Terumo Corporation. K.K. is an endowed chair sponsored by Terumo Corporation.

### References

1. Imamura T, Kinugawa K, Hatano M, Fujino T, Inaba T, Maki H, et al. Status 2 patients had poor prognosis without mechanical circulatory support. *Circ J* 2014; **78:** 1396–1404.
2. Sakaguchi T, Matsumiya G, Yoshioka D, Miyagawa S, Nishi H, Yoshikawa Y, et al. DuraHeart™ magnetically levitated left ventricular assist device: Osaka University experience. *Circ J* 2013; **77:** 1736–1741.
3. Sanganalmath SK, Bolli R. Cell therapy for heart failure: A comprehensive overview of experimental and clinical studies, current challenges, and future directions. *Circ Res* 2013; **113:** 810–834.
4. Dib N, McCarthy P, Campbell A, Yeager M, Pagani FD, Wright S, et al. Feasibility and safety of autologous myoblast transplantation in patients with ischemic cardiomyopathy. *Cell Transplant* 2005; **14:** 11–19.
5. Duckers HJ, Houtgraaf J, Hehrlein C, Schofer J, Waltenberger J, Gershlick A, et al. Final results of a phase IIa, randomised, open-label trial to evaluate the percutaneous intramyocardial transplantation of autologous skeletal myoblasts in congestive heart failure patients: The SEISMIC trial. *EuroIntervention* 2011; **6:** 805–812.
6. Menasché P, Alfieri O, Janssens S, McKenna W, Reichenspurner H, Trinquart L, et al. The Myoblast Autologous Grafting in Ischemic Cardiomyopathy (MAGIC) trial: First randomized placebo-controlled study of myoblast transplantation. *Circulation* 2008; **117:** 1189–1200.
7. Miyagawa S, Saito A, Sakaguchi T, Yoshikawa Y, Yamauchi T, Imanishi Y, et al. Impaired myocardium regeneration with skeletal cell sheets: A preclinical trial for tissue-engineered regeneration therapy. *Transplantation* 2010; **90:** 364–372.
8. Kondoh H, Sawa Y, Miyagawa S, Sakakida-Kitagawa S, Memon IA, Kawaguchi N, et al. Longer preservation of cardiac performance by sheet-shaped myoblast implantation in dilated cardiomyopathic hamsters. *Cardiovasc Res* 2006; **69:** 466–475.
9. Hata H, Matsumiya G, Miyagawa S, Kondoh H, Kawaguchi N, Matsuura N, et al. Grafted skeletal myoblast sheets attenuate myocardial remodeling in pacing-induced canine heart failure model. *J Thorac Cardiovasc Surg* 2006; **132:** 918–924.
10. Memon IA, Sawa Y, Fukushima N, Matsumiya G, Miyagawa S, Taketani S, et al. Repair of impaired myocardium by means of implantation of engineered autologous myoblast sheets. *J Thorac Cardiovasc Surg* 2005; **130:** 1333–1341.
11. Shudo Y, Miyagawa S, Nakatani S, Fukushima S, Sakaguchi T, Saito A, et al. Myocardial layer-specific effect of myoblast cell-sheet implantation evaluated by tissue strain imaging. *Circ J* 2013; **77:** 1063–1072.
12. Sawa Y, Miyagawa S, Sakaguchi T, Fujita T, Matsuyama A, Saito A, et al. Tissue engineered myoblast sheets improved cardiac function sufficiently to discontinue LVAS in a patient with DCM: Report of a case. *Surg Today* 2012; **42:** 181–184.
13. Jessup M, Greenberg B, Mancini D, Cappola T, Pauly DF, Jaski B, et al; Calcium Upregulation by Percutaneous Administration of Gene Therapy in Cardiac Disease (CUPID) Investigators. Calcium Upregulation by Percutaneous Administration of Gene Therapy in Cardiac Disease (CUPID): A phase 2 trial of intracoronary gene therapy of sarcoplasmic reticulum $Ca^{2+}$-ATPase in patients with advanced heart failure. *Circulation* 2011; **124:** 304–313.
14. Shiba N, Nochioka K, Miura M, Kohno H, Shimokawa H; CHART-2 Investigators. Trend of westernization of etiology and clinical characteristics of heart failure patients in Japan: First report from the CHART-2 study. *Circ J* 2011; **75:** 823–833.
15. US Food and Drug Administration. Guidance for industry: Cellular therapy for cardiac disease. FDA, MD, October 2010. Available from www.fda.gov [Guidance, Compliance & Regulatory Information] (accessed April 9, 2015).
16. Revision of "Guidelines on Clinical Evaluation of Drugs to Treat Heart Failure", Notification No. 0329 [18] of the Evaluation and Licensing Division, Pharmaceutical and Food Safety Bureau, March 29, 2011. Available from: http://www.pmda.go.jp/files/000157362.pdf (accessed April 9, 2015).
17. Hare JM, Bolli R, Cooke JP, Gordon DJ, Henry TD, Perin EC, et al. Cardiovascular Cell Therapy Research Network. Phase II clinical research design in cardiology: Learning the right lessons too well: Observations and recommendations from the Cardiovascular Cell Therapy Research Network (CCTRN). *Circulation* 2013; **127:** 1630–1635.
18. Menasché P, Hagège AA, Vilquin JT, Desnos M, Abergel E, Pouzet B, et al. Autologous skeletal myoblast transplantation for severe postinfarction left ventricular dysfunction. *J Am Coll Cardiol* 2003; **41:** 1078–1083.
19. Narita T, Shintani Y, Ikebe C, Kaneko M, Harada N, Tshuma N, et al. The use of cell-sheet technique eliminates arrhythmogenicity of skeletal myoblast-based therapy to the heart with enhanced therapeutic effects. *Int J Cardiol* 2013; **168:** 261–269.

### Supplementary Files

**Supplementary File 1**

**Table S1.** Inclusion and exclusion criteria for study of cell sheet transplantation

**Table S2.** Observation and test items and schedule of study of cell sheet transplantation

**Figure S1.** Serial change in B-type natriuretic peptide from baseline to 26 weeks after cell sheet transplantation.

Please find supplementary file(s);
http://dx.doi.org/10.1253/circj.CJ-15-0243

# Cell-sheet Therapy With Omentopexy Promotes Arteriogenesis and Improves Coronary Circulation Physiology in Failing Heart

Satoshi Kainuma[1], Shigeru Miyagawa[1], Satsuki Fukushima[1], James Pearson[2], Yi Ching Chen[2], Atsuhiro Saito[1], Akima Harada[1], Motoko Shiozaki[1], Hiroko Iseoka[1], Tadashi Watabe[3], Hiroshi Watabe[3], Genki Horitsugi[4], Mana Ishibashi[4], Hayato Ikeda[4], Hirotsugu Tsuchimochi[5], Takashi Sonobe[5], Yutaka Fujii[5], Hisamichi Naito[6], Keiji Umetani[7], Tatsuya Shimizu[8], Teruo Okano[8], Eiji Kobayashi[9], Takashi Daimon[10], Takayoshi Ueno[1], Toru Kuratani[1], Koichi Toda[1], Nobuyuki Takakura[6], Jun Hatazawa[4], Mikiyasu Shirai[5] and Yoshiki Sawa[1]

*[1]Department of Cardiovascular Surgery, Osaka University Graduate School of Medicine, Osaka, Japan; [2]Monash Biomedical Imaging Facility and Department of Physiology, Monash University, Melbourne, Australia; [3]Department of Molecular Imaging in Medicine, Osaka University Graduate School of Medicine, Osaka, Japan; [4]Department of Nuclear Medicine and Tracer Kinetics, Osaka University Graduate School of Medicine, Osaka, Japan; [5]Department of Cardiac Physiology, National Cerebral and Cardiovascular Center Research Institute, Osaka, Japan; [6]Department of Signal Transduction, Research Institute for Microbial Diseases, Osaka University, Osaka, Japan; [7]Japan Synchrotron Radiation Research Institute, Harima, Japan; [8]Institute of Advanced Biomedical Engineering and Science, Tokyo Women's Medical University, Tokyo, Japan; [9]Division of Organ Replacement Research, Center for Molecular Medicine, Jichi Medical School, Tochigi, Japan; [10]Department of Biostatistics, Hyogo College of Medicine, Hyogo, Japan*

Cell-sheet transplantation induces angiogenesis for chronic myocardial infarction (MI), though insufficient capillary maturation and paucity of arteriogenesis may limit its therapeutic effects. Omentum has been used clinically to promote revascularization and healing of ischemic tissues. We hypothesized that cell-sheet transplantation covered with an omentum-flap would effectively establish mature blood vessels and improve coronary microcirculation physiology, enhancing the therapeutic effects of cell-sheet therapy. Rats were divided into four groups after coronary ligation; skeletal myoblast cell-sheet plus omentum-flap (combined), cell-sheet only, omentum-flap only, and sham operation. At 4 weeks after the treatment, the combined group showed attenuated cardiac hypertrophy and fibrosis, and a greater amount of functionally ($CD31^+$/$lectin^+$) and structurally ($CD31^+$/$\alpha$-$SMA^+$) mature blood vessels, along with myocardial upregulation of relevant genes. Synchrotron-based microangiography revealed that the combined procedure increased vascularization in resistance arterial vessels with better dilatory responses to endothelium-dependent agents. Serial $^{13}$N-ammonia PET showed better global coronary flow reserve in the combined group, mainly attributed to improvement in the basal left ventricle. Consequently, the combined group had sustained improvements in cardiac function parameters and better functional capacity. Cell-sheet transplantation with an omentum-flap better promoted arteriogenesis and improved coronary microcirculation physiology in ischemic myocardium, leading to potent functional recovery in the failing heart.

*Received 27 August 2014; accepted 16 November 2014; advance online publication 13 January 2015. doi:10.1038/mt.2014.225*

## INTRODUCTION

Heart failure following myocardial infarction (MI) is a major cause of death and disability worldwide. Despite advances in drug and device therapy, recovery of cardiac function and prevention of transition to heart failure in MI patients remain unsatisfactory, indicating the need for development of novel therapeutic alternatives.[1] Myocardial regenerative therapy with cell-sheet transplantation has been shown to induce angiogenesis via paracrine effects in a chronic MI model.[2,3] However, the proangiogenic effect of the stand-alone cell-sheet treatment may be insufficient to fully relief ischemia in the chronic MI heart that involves a large territory of the left ventricle (LV), since the coronary inflow of the ischemic/infarct myocardium is dependent upon collateral arteries from other territories.[4,5] In addition, microvascular dysfunction is present in critical chronic MI heart across a wide range of the peripheral coronary tree.[6] This highlights the need for a comprehensive understanding of the mechanism of angiogenesis induced by a cell-sheet therapy in ischemic hearts.

For successful therapeutic neovascularization of ischemic tissues, it is essential to induce robust angiogenic responses (angiogenesis), and establish functionally and structurally mature arterial vascular networks (arteriogenesis) that show long-term stability and control perfusion.[5] Establishment of mature vessels is a complex process that requires several angiogenic factors to stimulate vessel sprouting and remodeling (endothelial tubulogenesis accompanied with a pericyte recruitment) of the primitive vascular network. Endothelial vasodilator function of coronary microvessels (resistance arterial vessels) is also an important determinant of myocardial perfusion in response to increased myocardial oxygen demand, playing a critical role in neovascular therapies.[6–8] The attenuated therapeutic effects observed in the previous clinical trials were caused by multiple factors including

*Correspondence: Yoshiki Sawa, Chairman of Department of Cardiovascular Surgery, Osaka University Graduate School of Medicine, 2-2-E1, Yamadaoka, Suita, Osaka 565–0871, Japan. E-mail: sawa-p@surg1.med.osaka-u.ac.jp*

generation of unstable blood vessels that regress over time or functionally immature vessels accompanied with endothelial dysfunction in ischemic areas.[5,9]

The omentum (OM), historically used in surgical revascularization for patients with ischemic heart disease, is also known to release a number of angiogenic cytokines and attenuate inflammation.[10–14] In addition, the gastroepiploic artery involved in the OM-flap can play an important role as an extracardiac blood source with high perfusion capacity for developing effective collateral vessels for advanced coronary artery disease. We established a combination strategy of cell-sheet transplantation covered with a pedicle OM-flap in porcine models, allowing us to implant large numbers of cells and improve cell survival.[13,14] However, data are scarce regarding the therapeutic effects of such combined treatment on vessel maturity and coronary microcirculation physiology in ischemic territory. We hypothesized that cell-sheet transplantation with a pedicle OM-flap will better promote arteriogenesis and stabilize blood vessels in ischemic myocardium along with improved coronary microcirculation physiology, consequently enhancing the therapeutic effects of cell-sheet therapy. Herein, we focused on vessel maturation induced by cell-sheet therapy with an OM-flap and evaluated the physiological benefits in coronary microcirculation utilizing modern modalities such as *in vivo* synchrotron-based microangiography and positron emission tomography (PET).

## RESULTS

### Histological analysis of host myocardium

Four weeks after treatment, myocardial structural components, collagen accumulation and cardiomyocyte hypertrophy, were assessed by hematoxylin-eosin, Masson trichrome, and Periodic acid-Schiff staining ($n$ = 11 for each group). LV myocardial structure was better maintained in the combined group as compared with the others (**Figure 1c**). The combined group had a significantly thickened anterior LV wall (anterior wall thickness, control 392 ± 31 versus combined 912 ± 34 versus sheet-only 688 ± 27 versus OM-only 500 ± 28 μm) (**Figure 1d**). That group also had a significantly attenuated collagen accumulation (percent fibrosis, 18 ± 1 versus 8 ± 4 versus 13 ± 6 versus 14 ± 1%, respectively) (**Figure 1e**) and cardiac hypertrophy (myocyte size, 23 ± 1 versus 16 ± 1 versus 20 ± 3 versus 21 ± 2 μm, respectively) (**Figure 1f**) in the peri-infarct regions (ANOVA $P < 0.001$ for all).

### Gene expressions in peri-infarct myocardium during acute treatment phase

The myocardial gene expressions related to angiogenesis, vessel maturation, and anti-inflammation were analyzed at 3 days after each treatment using real-time PCR ($n$ = 6 for each group). As compared to the others, the combined group showed substantially higher gene expressions of *vascular endothelial growth factor (VEGF)-A*, *VEGF receptor-1*, *VEGF receptor-2*, *Akt-1*, *platelet-derived growth factor (PDGF)-β*, *angiopoietin (Ang)-1*, *Tie-2*, *vascular endothelial (VE)-cadherin*, *platelet endothelial cell adhesion molecule (PECAM)-1*, and *stromal cell-derived factor (SDF)-1* in peri-infarct myocardium at the early stage of transplantation (**Figure 2**).

### Vessel recruitment in transplanted cell-sheets and donor cell survial

To evaluate the effect of adding OM-flap to the cell-sheet therapy on the vessel recruitment (angiogenesis) in the transplanted area that should be related to the donor cell survival, we serially assessed the number of functional blood vessels with patent endothelial layers (CD31/lectin double-positive cells) in the transplanted area of the sheet-only and combined groups at 3, 7, and 28 days after each treatment ($n$ = 6 for each group and each time point) (**Figure 3a–f**). At 3 days after treatment, in the sheet-only group, several blood vessels were just located at the border between the sheet and infarct area (**Figure 3a**), whereas a large number of functional vessels was detected proximal to the border between the cell-sheet and OM and within the sheet in the combined group (**Figure 3d**), suggesting that the cell-sheet received blood supply directly from the infarct myocardium and OM. Consequently, the combined group had greater numbers of functional blood vessels in the cell-sheet than the sheet-only group at any follow-up point, although both groups showed steady decrease in the number of vessels during the 28 days (**Figure 3g**).

The quantitative assessments of the donor (GFP-positive) cell presence were also serially performed to elucidate the donor cell dynamics in the sheet-only (**Figure 3a–c**) and combined (**Figure 3d–f**) groups. We traced the transplanted donor cells and found that there was no significant difference in the engrafted area at 3 days after transplantation between the groups, while the subsequent changes in each group were apparently distinctive (**Figure 3h**). During the 7days after the treatment, the amount of decrease in the engrafted area was substantially smaller in the combined group than that in the sheet-only group, resulting in 4.3-fold increased retention of donor cells in the former group. This led to the greater donor cell presence in the combined group persistently (at least until day 28), which was consistent with the amount of vessel recruitment in the cell-sheet.

### Vessel remodeling and maturation in peri-infarct myocardium

We serially assessed neovascular vessel maturity in peri-infarct areas at 3 ($n$ = 6 for each group) and 28 days ($n$ = 11 for each group) after treatment (**Figure 4**). Vessel density and structural maturity were quantified as the number of CD31 positive and CD31/α-smooth muscle actin (SMA) double-positive vessels per mm$^2$, respectively. A maturation index was calculated as the percentage of CD31/α-SMA double-positive vessels to total vessel number. Functionally mature vessels with patent endothelial layers were assessed by lectin injection, which binds uniformly and rapidly to the luminal surface of endothelium, thus labeling patent blood vessels. Vessels positive for CD31 but negative for lectin were regarded as functionally immature and undergoing regression, or that had lost patency.[15,16]

In general, α-SMA signals were located at the outer edges of CD31 staining, indicating pericyte attachment to newly formed endothelium. Three days after treatment, there was no difference in number of CD31-positive cells among the groups, though the combined group showed a trend of greater number of functional blood vessels with patent endothelial layers (CD31/lectin double-positive) and structurally (CD31/α-SMA double-positive) mature vessels, with a higher maturation index (**Figure 4a–g**). Notably, the percentage without lectin staining (CD31$^+$/lectin$^-$) was significantly smaller in the combined group.

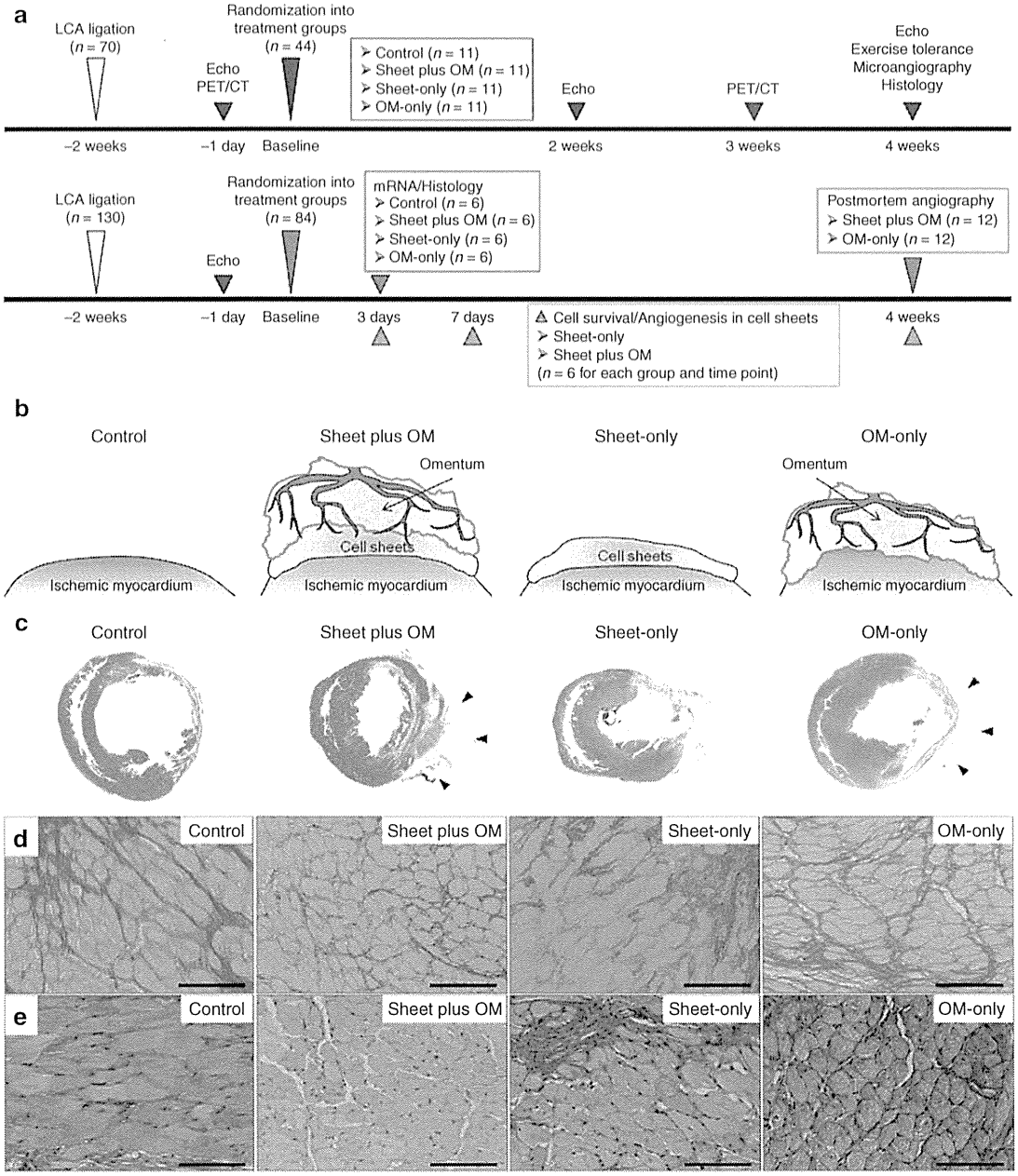


Figure 1 (**a**) Experimental protocols. (**b**) Procedural schemes for treatment groups. (**c**) Macroscopic images of HE-stained whole sections of the left ventricle and (**d**) anterior wall thickness (40×, scale bar = 1,000 μm). Black arrows indicate the omentum tissue. Photomicrographs of Sirius red- (**e**) and periodic acid-Schiff-stained (**f**) sections of peri-infarct myocardium (400×, scale bar = 100 μm) ($n$ = 11 for each group).

The number of endothelial (CD31 positive) cells in the control and single treatment groups decreased with time, while that in the combined remained unchanged. Consequently, the angiogenic effects induced in the latter were more profound at 28 days after treatment, with a significantly greater amount of mature vessels (Figure 4h–n).

## Number of resistance vessels and relative dilatory responses to endothelium-dependent stimulation in ischemic myocardium

To evaluate the effects of each treatment on microcirculation physiology in terms of relative dilatory responses to acetylcholine and dobutamine hydrochloride in the resistance vessels, synchrotron radiation microangiography was performed after 3 weeks after the treatment (control: $n$ = 11, combined: $n$ = 11, cell-sheet: $n$ = 5, OM: $n$ = 6). Using iodinated agents, coronary microcirculation in ischemic areas was clearly visualized in anesthetized closed-chest rats (Figure 5a). Vessel internal diameter (ID) at baseline (before agent administration) tended to decrease according to branching order and differed among the groups with larger first branching order arteries observed in the combined group (Figure 5b). Moreover, the combined group had a greater number of third and fourth branching order arterial vessels (resistance arterial vessels) at baseline (Figure 5c).

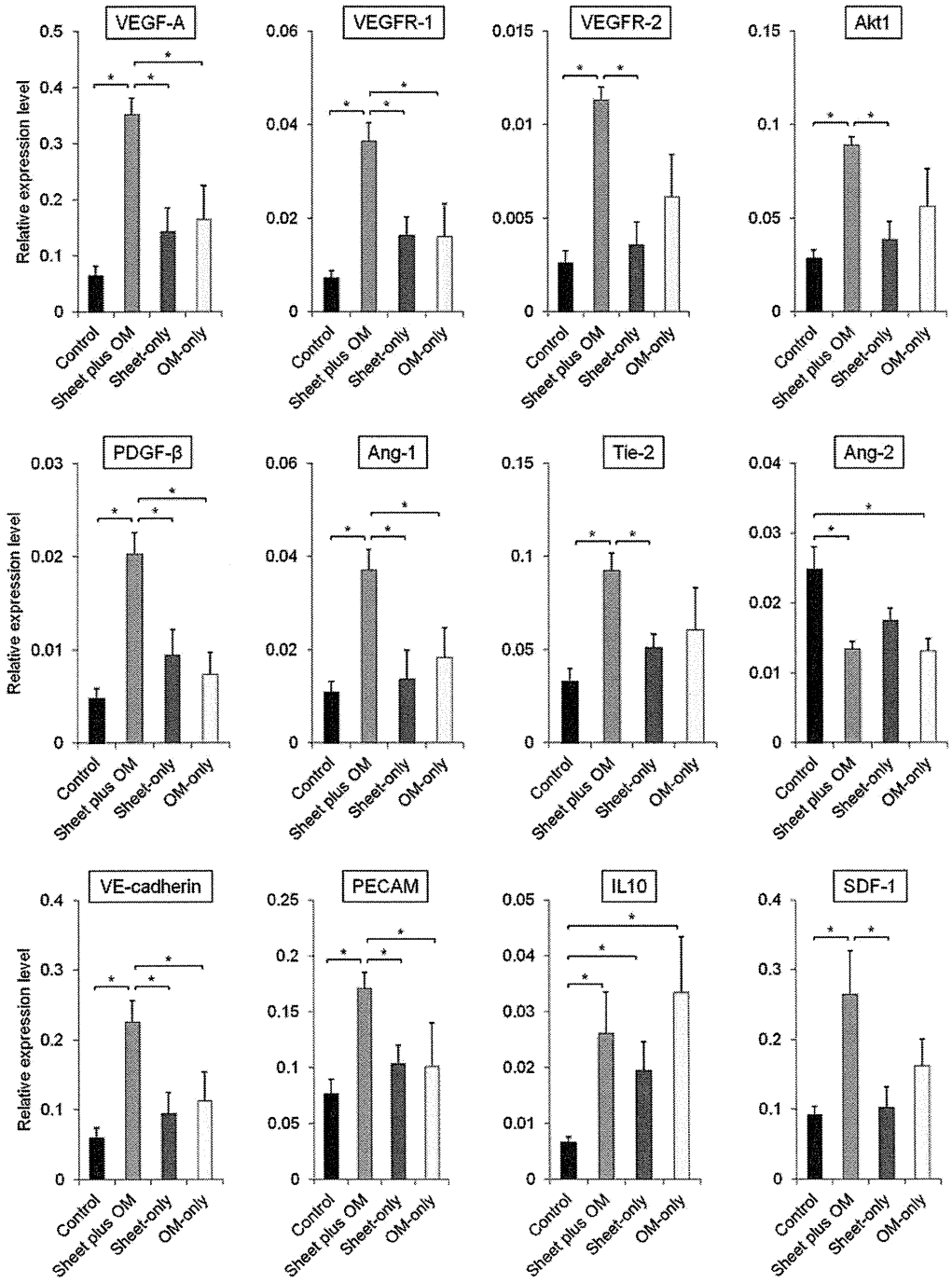


Figure 2 Quantitative reverse transcription PCR showing gene expressions related to angiogenesis, vessel maturation, and anti-inflammation in peri-infarct myocardium 3 days after treatment ($n = 6$ for each group) (*$P < 0.05$). Data were normalized to β-actin expression level. As compared to the others, the combined group showed substantially higher gene expressions associated with angiogenesis, vessel remodeling and anti-inflammation in peri-infarct myocardium at 3 days after treatment.

Acetylcholine-mediated dilation in the third and fourth branching orders was significantly different among the groups. The mean caliber changes in response to acetylcholine in the combined group were 28±8% and 32±8% for the third and fourth order branches respectively, which were greater than in the others (Figure 5d). Similarly, the mean caliber changes in response to dobutamine hydrochloride in the combined group were 31±7% and 34±7%, respectively, which were greater than in the others (Figure 5e).

The distributions of individual segment caliber changes in response to acetylcholine are described in **Supplementary Figure S1**. The control group had a relatively high frequency of third and fourth branching order arterial vessels showing localized segmental vasoconstriction (ID constriction >5% of baseline). The frequency of abnormal vasoconstriction with acetylcholine in the control group was about eight- and fourfold for the third and fourth branching order, respectively, as compared

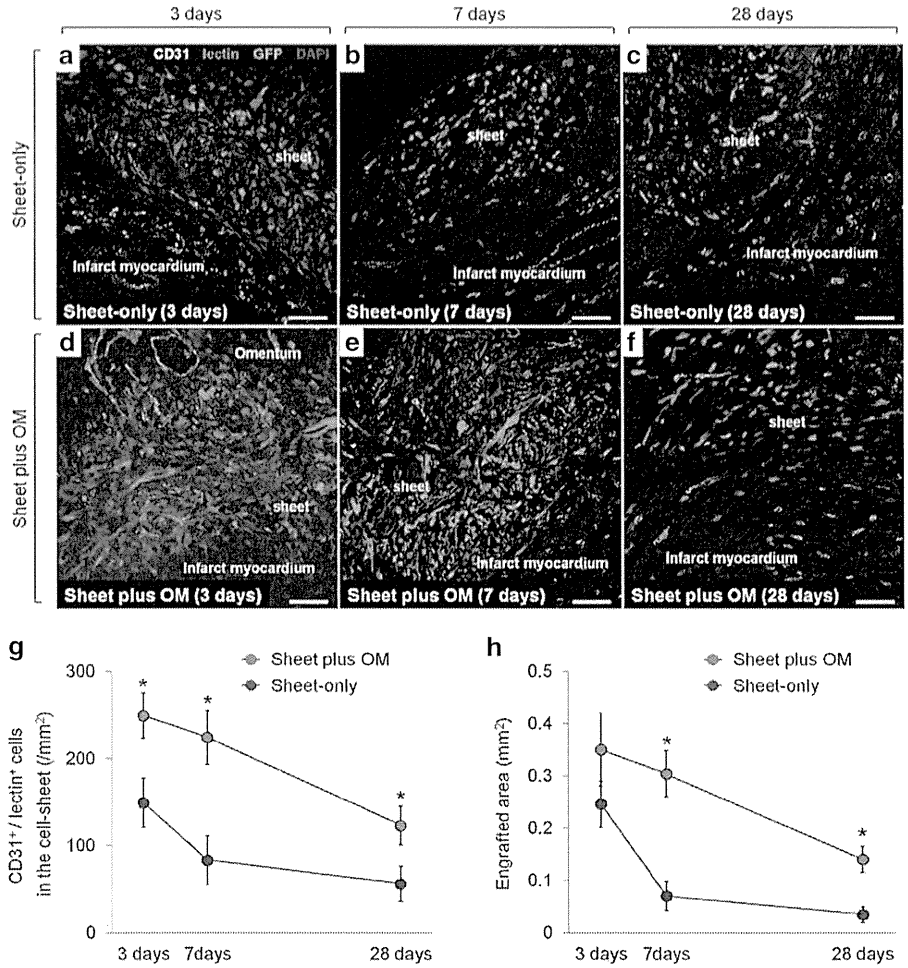


Figure 3 Serial representative images of functional blood vessels with patent endothelial layers (CD31/lectin double-positive) vessels in the transplanted donor (GFP-positive) cells in sheet-only (**a**–**c**) and combined groups (**d**–**f**) at 3, 7, and 28 days after each treatment (200×, scale bar = 100 μm). Quantitative analyses of functionally mature vessels in the transplanted area (**g**) and the donor (GFP-positive) cell presence (**h**) at 3, 7, and 28 days after each treatment ($n = 6$ for each group and each time point) (* $P < 0.05$ versus sheet-only group). At 3 days after treatment, in the sheet-only group, several blood vessels were just located at the border between the sheet and infarct area (**a**), whereas a large number of functional vessels was detected proximal to the border between the cell-sheet and OM and within the sheet in the combined group (**d**). Consequently, the combined group had greater numbers of functional blood vessels in the cell-sheet than the sheet-only group at any follow-up point (**g**). There was no significant difference in the engrafted area at 3 days after transplantation between the groups, while the subsequent changes in each group were apparently distinctive (**h**). During the 7 days after the treatment, the amount of decrease in the engrafted area was substantially smaller in the combined group than that in the sheet-only group, resulting in 4.3-fold increased retention of donor cells in the former group. This led to the greater donor cell presence in the combined group persistently (at least until day 28), which was consistent with the amount of vessel recruitment in the cell-sheet.

with the combined group (third order: control 49% versus combined 6% versus sheet-only 22% versus OM-only 25%; fourth order: control 18% versus combined 4% versus sheet-only 13% versus OM-only 17%).

## Global and regional changes in myocardial blood flow and coronary flow reserve

To evaluate global and regional myocardial blood flow (MBF), and coronary flow reserve (CFR), $^{13}$N-ammonia PET measurements were serially performed 1 day before and 3 weeks after the treatments (control: $n = 5$, combined: $n = 8$, cell-sheet: $n = 7$, OM: $n = 7$) (Figure 6a–f). In normal rats used for the validation study, global MBF at rest and during stress was 5.1 ± 0.5 and 7.1 ± 1.3 ml/min/g respectively, while global CFR was 1.4 ± 0.3.

Two weeks after coronary ligation (before treatment), global MBF at rest and during stress were substantially decreased in all groups, with no significant differences. Similarly, global CFR was not different among the groups. Three weeks after treatment, global MBF at rest was not different, while that during stress was significantly greater in the combined and single treatment groups as compared to the control (control 2.5 ± 0.4 versus combined 3.8 ± 0.6 versus sheet-only 3.3 ± 0.5 versus OM-only 3.8 ± 0.3, respectively, ANOVA p=0.0003). Postoperative global CFR was also substantially higher in the treatment groups as compared with the control (control 1.1 ± 0.2 versus combined 1.4 ± 0.2 versus sheet-only 1.4 ± 0.2 versus OM-only 1.4 ± 0.2, respectively, ANOVA p=0.015).

With regard to the magnitude of change in the global CFR (pre- versus post-treatment), the combined group offered the

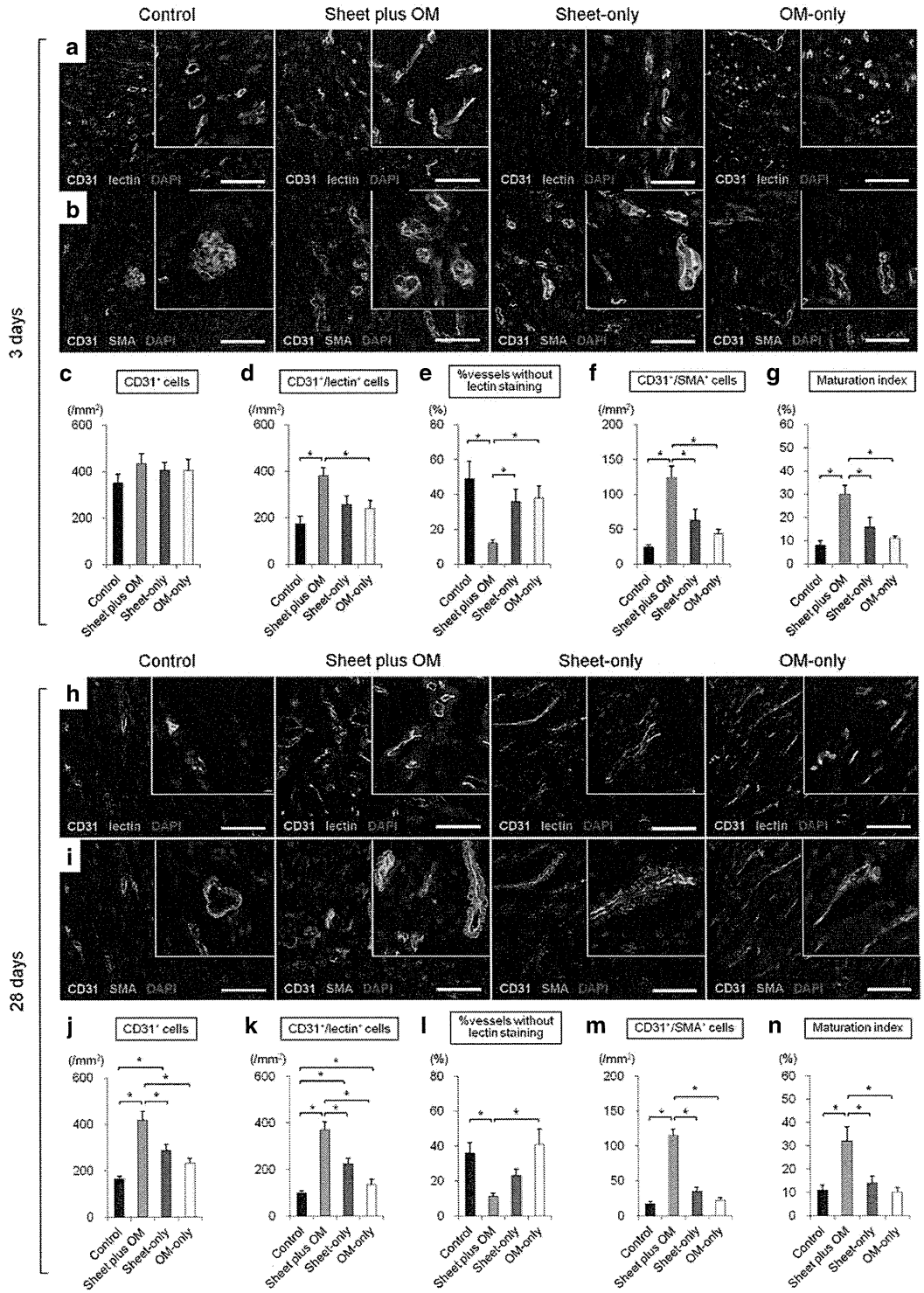


Figure 4 Immunohistochemical analyses of functionality (patency) and vessel maturation observed in peri-infarct myocardium at 3 ($n = 6$ for each group) (**a–g**) and 28 ($n = 11$ for each group) (**h–n**) days after treatments (* $P < 0.05$). Representative CD31/lectin and CD31/α-SMA staining at 3 (**a,b**) and 28 (**h,i**) days after treatments (400×, scale bar= 100 μm). Three days after treatment, there was no difference in number of CD31-positive cells among the groups, though the combined group showed a trend of greater number of functional blood vessels with patent endothelial layers (CD31/lectin double-positive) and structurally (CD31/α-SMA double-positive) mature vessels, with a higher maturation index (**c–g**). Notably, the percentage without lectin staining ($CD31^+/lectin^-$) was significantly smaller in the combined group. The number of endothelial (CD31 positive) cells in the control and single treatment groups decreased with time, while that in the combined remained unchanged. Consequently, the angiogenic effects induced in the latter were more profound at 28 days after treatment, with a significantly greater amount of mature vessels (**j–n**).

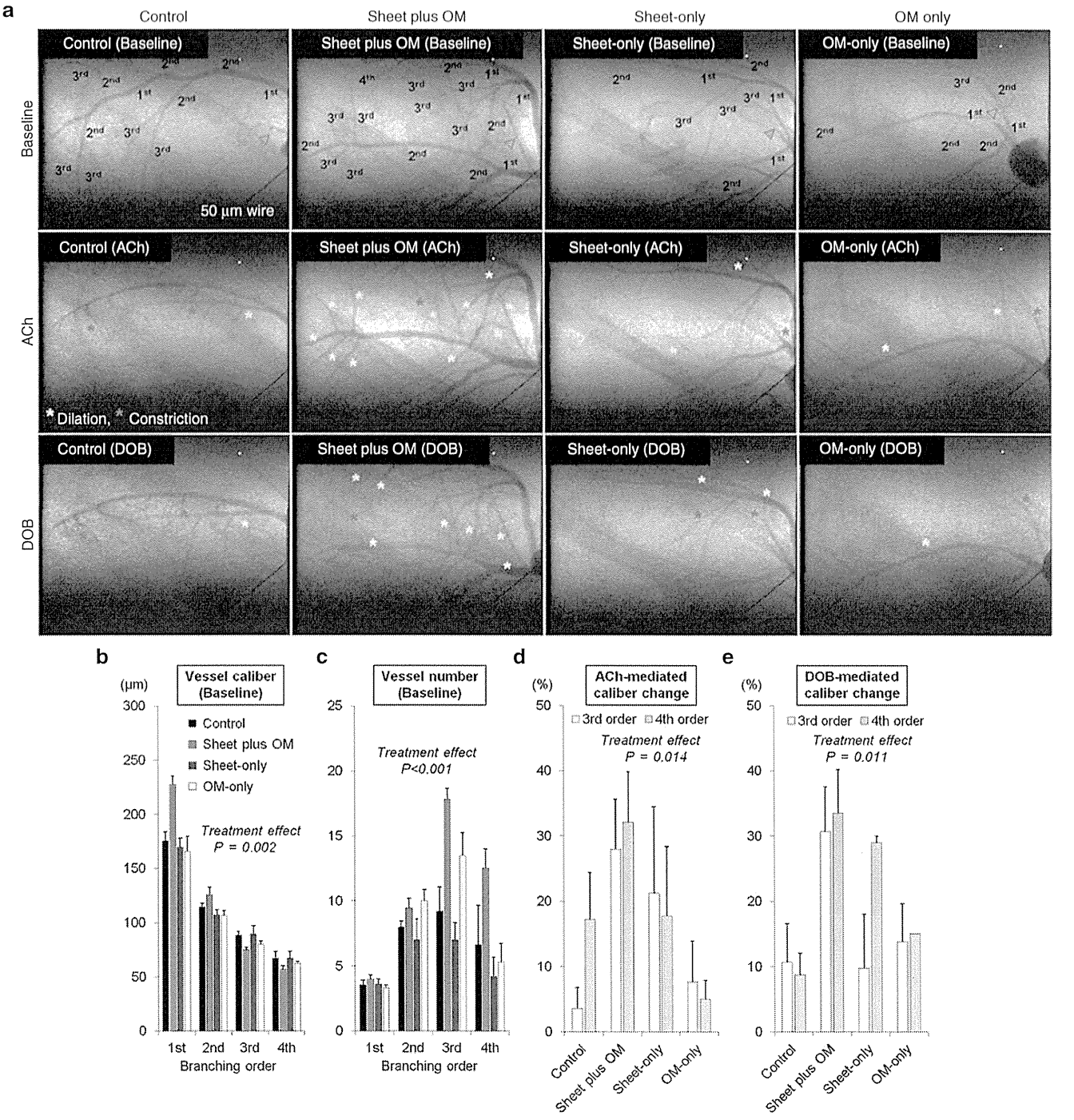


Figure 5 Synchrotron radiation microangiography was performed to evaluate vessel number and caliber and relative dilatory responses to acetylcholine and dobutamine hydrochloride in resistance vessels (control: $n = 11$, combined: $n = 11$, cell-sheet: $n = 5$, OM: $n = 6$). Using iodinated agents, coronary microcirculation in ischemic areas was clearly visualized in anesthetized closed-chest rats. Representative angiogram frames for all treatment groups at baseline, and in response to acetylcholine and dobutamine hydrochloride (**a**). Yellow and red asterisks indicate vessels showing dilation and constriction in response to acetylcholine and dobutamine hydrochloride, respectively. Quantitative analyses of (**b**) vessel internal diameter and (**c**) visible vessel number at baseline according to branching order. Vessel internal diameter at baseline (before agent administration) tended to decrease according to branching order and differed among the groups with larger first branching order arteries observed in the combined group (**b**). Moreover, the combined group had a greater number of third and fourth branching order arterial vessels (resistance arterial vessels) at baseline (**c**). Mean caliber changes in response to (**d**) acetylcholine and (**e**) dobutamine hydrochloride. Acetylcholine-mediated dilation in the third and fourth branching orders was significantly different among the groups. The mean caliber changes in response to acetylcholine in the combined group were 28 ± 8% and 32 ± 8% for the third and fourth order branches respectively, which were greater than in the others (**d**). Similarly, the mean caliber changes in response to dobutamine hydrochloride in the combined group were 31 ± 7% and 34 ± 7%, respectively, which were greater than in the others (**e**).

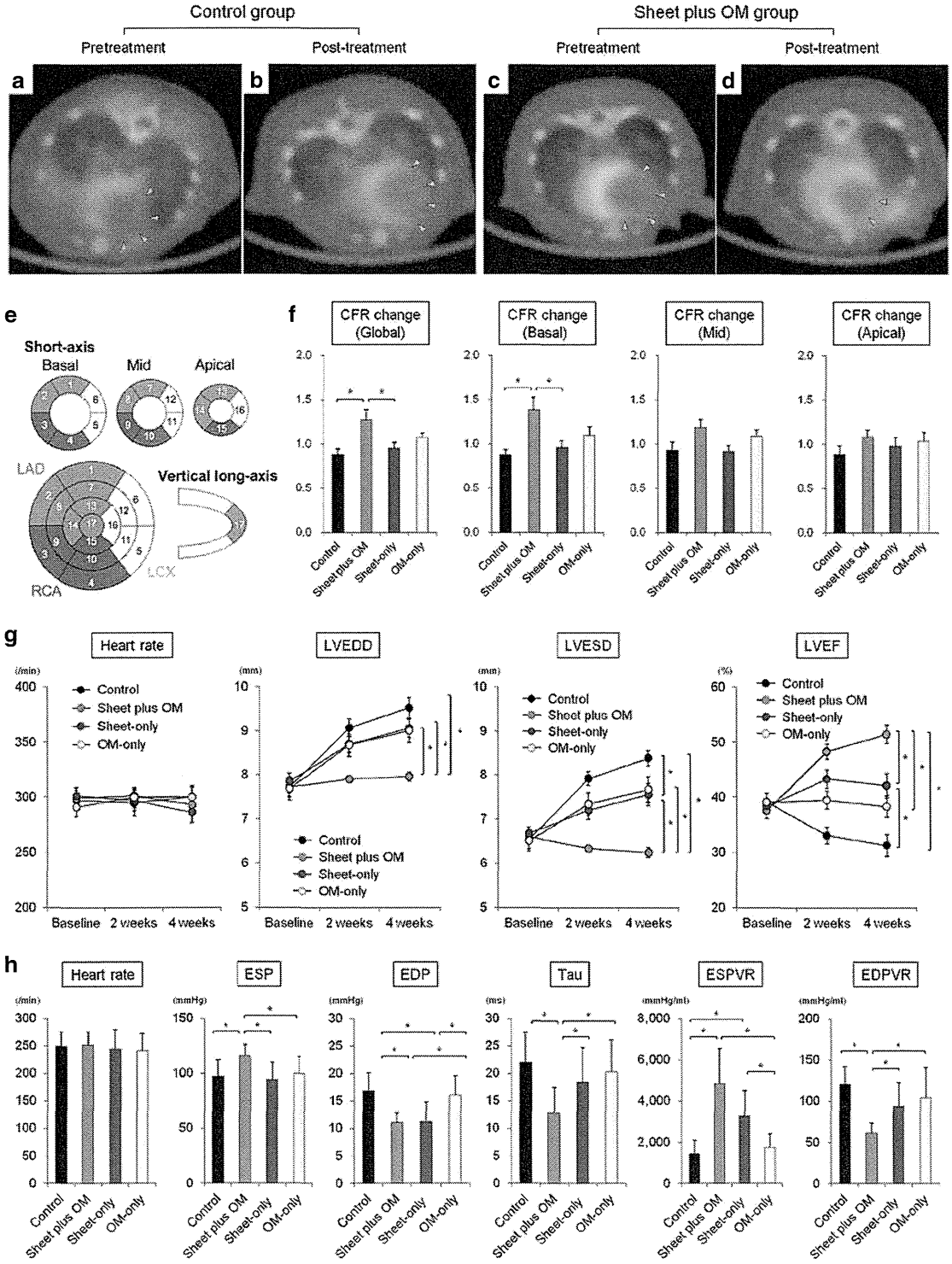


Figure 6 Representative serial PET/CT fusion images of $^{13}$N-$NH_3$ PET during stress in control (a,b) and combined (c,d) groups. Recovery of MBF in large portion of basal left ventricle (anterior and lateral segments) was observed in the combined but not control group (green triangles). Quantitative analyses of changes in CFR calculated as a ratio of post-treatment to pretreatment CFR in global, basal, mid, and apical LV segments (control: $n = 5$, combined: $n = 8$, cell-sheet: $n = 7$, OM: $n = 7$) (*$P < 0.05$) (**e,f**). The combined group offered the most remarkable improvement in the global CFR, as evidenced by a higher ratio of post- to pretreatment CFR. Notably, that beneficial change was mainly caused by significant improvement in the basal left ventricle. CFR, coronary flow reserve; MBF, myocardial blood flow. (**g**) Serial assessments of cardiac function parameters at baseline (before treatment), and 2 and 4 weeks after treatments (*$P < 0.05$). In the combined group, remarkable improvements in LV function parameters occurred promptly and were sustained for up to 4 weeks, resulting in significantly smaller LV dimensions and greater LV ejection fraction as compared with other treatment groups. (**h**) Quantitative analyses of hemodynamic function parameters for each treatment (*$P < 0.05$). The basic hemodynamic indices revealed that LV end-systolic pressure was higher, whereas LV end-diastolic pressure and time constant were lower in the combined group as compared to the others. Pressure–volume loop analysis revealed that end-systolic pressure–volume relationship was higher, while end-diastolic pressure–volume relationship was lower in the combined group.

most remarkable improvement in the global CFR, as evidenced by a higher ratio of post- to pre-treatment CFR. Notably, that beneficial change was mainly caused by significant improvement in the basal left ventricle (control 0.9 ± 0.1 versus combined 1.4 ± 0.4 versus sheet-only 1.0 ± 0.1 versus OM-only 1.1 ± 0.1, respectively, ANOVA $P = 0.012$) (Figure 6e,f).

### Global LV function and hemodynamic performance

The cardiac function was evaluated by echocardiography before (at baseline) and 2 and 4 weeks after each treatment ($n = 11$ for each group) (Figure 6 g,h). Two weeks after left coronary artery ligation, severe dilatation of the LV chamber and severe systolic dysfunction were observed, with no significant differences among the groups (Figure 6g). In the control, LV dimensions increased and LV ejection fraction deteriorated in a time-dependent manner, suggesting progressive LV remodeling. In the sheet-only and OM-only groups, LV ejection fraction initially improved, then tended to deteriorate in association with gradual LV dilatation. In the combined group, remarkable improvements in LV function parameters occurred promptly and were sustained for up to 4 weeks, resulting in significantly smaller LV dimensions and greater LV ejection fraction as compared with other treatment groups.

Consistently, the basic hemodynamic indices revealed that LV end-systolic pressure was higher, whereas LV end-diastolic pressure and time constant were lower in the combined group as compared to the others. Load-independent parameters assessed by pressure–volume loop analysis revealed that end-systolic pressure–volume relationship was higher, while end-diastolic pressure–volume relationship was lower in the combined group (Figure 6h). These results confirmed that cell-sheet therapy combined with OM-flap improved the therapeutic effects of single treatment group (cell-sheet only or OM-flap only) for the treatment of chronic MI.

### Functional capacity assessment

There was no difference in running distance at 4 rpm (control 125 ± 15 versus combined 148 ± 9 versus sheet-only 133 ± 10 versus OM-only 135 ± 15 m, ANOVA $P = 0.63$) ($n = 11$ in each). In contrast, the combined group showed more improved functional capacity in terms of longer running distance at 8 rpm (54 ± 5 versus 178 ± 17 versus 81 ± 10 versus 76 ± 7 m, respectively, ANOVA $P < 0.001$).

### Angiographic assessment of communication between coronary arteries and pedicle omentum

Communication between the coronary arteries and branches of the gastroepiploic artery in the OM specimens was evaluated using three different methods with a different series of OM-only and combined group animals ($n = 12$ in each) (Figure 1a).

A postmortem angiography examination from the aortic root was performed to verify antegrade flow from the OM into the heart in the combined and OM-only groups ($n = 4$ for each group). In the combined group, aortography revealed that the gastroepiploic artery branches feeding the OM expanded into the heart, and established several tight junctions between the native coronary arteries and OM (Figure 7a). In contrast, in the OM-only group, the gastroepiploic artery branches failed to penetrate the heart, accompanied by immature leaky collateral vessel formation between the coronary artery and OM, evidenced by considerable leakage of contrast agent (Figure 7b).

We selectively injected India ink into the celiac artery to visually and histologically confirm vessel communication between the pedicle OM and native coronary artery ($n = 4$ for each group). Numerous collaterals filled with India ink were clearly identified between the gastroepiploic artery and native coronary arteries in the combined group, while that was not seen in the OM-only group (data not shown) (Figure 7c–e). Histological analysis confirmed vessel communication between those in the combined group (Figure 7f,g).

Finally, a selective perfusion via aortic root and celiac artery using two different MICROFIL colors was performed ($n = 4$ for each group). In the combined group, MICROFIL solution injected in a retrograde manner into the aortic root (MV-117 Orange) was easily shown expanded into the OM to communicate with the gastroepiploic artery (Figure 7h). That solution injected into the celiac artery (MV-120 Blue) was also found to expand into the myocardium and communicated with native coronary arteries (Figure 7i). Those findings were not seen in the OM-only group (data not shown).

### Vessel migration into cell-sheet from host myocardium and omentum

To further confirm whether the OM- and host myocardium-derived endothelial cells migrated toward the cell-sheet, we established two types of parabiotic pair models ($n = 4$ for each).

In parabiotic pairs of wild-type MI rats that received transplantation of cell-sheets labeled with Cell Tracker TM Orange CMTMR followed by coverage with a GFP-transgenic rat oriented pedicle OM, a large number of OM-derived endothelial cells (isolectin/GFP double-positive cells) had migrated toward the cell-sheet (Figure 8a–d). Similarly, in another parabiotic pair of GFP-transgenic MI rats that received cell-sheet transplantation covered with a wild-type rat oriented pedicle OM, a large number of host myocardium-derived endothelial cells (isolectin/GFP double-positive cells) had migrated toward the cell-sheet (Figure 8e–h).

### Cell-sheet stimulated vascular cell migration

We performed an *in vitro* migration assay using HUVECs to evaluate the effects of skeletal myoblast cell-sheet derived growth factors on vessel recruitment (Figure 8i). The number of migrating cells was significantly greater in the 100% conditioned medium group, followed by the 10% conditioned medium and control groups, suggesting that SM cell-sheet derived growth factors stimulate vascular cell migration in a concentration-dependent manner (Figure 8j,k).

## DISCUSSION

The major findings of this study can be summarized as follows. As compared to the single treatment groups, the cell-sheet plus OM group showed (i) improved donor cell retention along with amplified angiogenesis in the cell-sheet through the follow-up (at least day 28), (ii) attenuated cardiac hypertrophy and

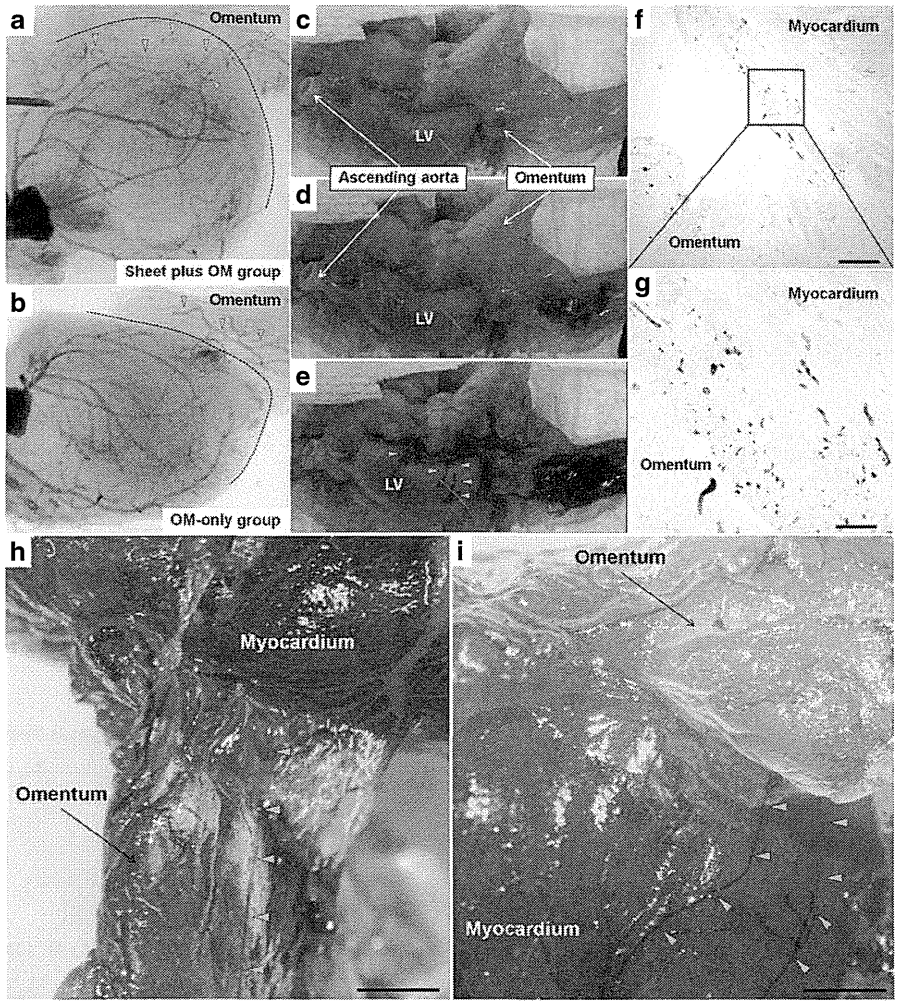


Figure 7 Communication between the coronary arteries and branches of the gastroepiploic artery was evaluated using three different methods with a different series of OM-only and combined group animals. A postmortem angiography examination from the aortic root in the combined (**a**) and OM-only (**b**) groups ($n = 4$ for each group). In the combined group, aortography revealed that the gastroepiploic artery branches feeding the OM expanded into the heart, and established several tight junctions between the native coronary arteries and OM (**a**). In contrast, in the OM-only group, the gastroepiploic artery branches failed to penetrate the heart, accompanied by immature leaky collateral vessel formation between the coronary artery and OM, evidenced by considerable leakage of contrast agent (red dotted circle) (**b**). Black dotted line indicates heart surface. Green triangles indicate the branches of the gastroepiploic artery. Selective India ink injection into the celiac artery to visually and histologically confirm vessel communication between the pedicle OM and native coronary artery ($n = 4$ for each group). Numerous collaterals filled with India ink were clearly identified between the gastroepiploic artery and native coronary arteries in the combined group (**c–e**), while that was not seen in the OM-only group (data not shown). Histological analysis confirmed vessel communication between those in the combined group (**f**: 40×, scale bar = 500 μm, **g**: 200×, scale bar = 100 μm). A selective perfusion via aortic root and celiac artery using two different MICROFIL colors ($n = 4$ for each group). In the combined group, MICROFIL solution injected in a retrograde manner into the aortic root (MV-117 Orange) was easily shown expanded into the OM to communicate with the gastroepiploic artery (**h**, 7.5×, scale bar = 2 mm). That solution injected into the celiac artery (MV-120 Blue) was also found to expand into the myocardium and communicated with native coronary arteries (**i**, 7.5×, scale bar = 2 mm). Those findings were not seen in the OM-only group (data not shown). Green triangles show visible vessel communication in the OM-flap (**h**) and host myocardium (**i**).

fibrosis, and a greater amount of functionally and structurally mature blood vessels in the ischemic myocardium, along with myocardial upregulation of relevant genes, (iii) increased vascularization in resistance arterial vessels with better dilatory responses to endothelium-dependent agents, (iv) more remarkable improvement in the global CFR, mainly caused by significant improvement in the basal left ventricle, (v) sustained improvements in cardiac function parameters and better functional capacity, and (vi) creation of robust vascular communication between the OM and native coronary arteries, shown by *in vivo* angiography.

The retention, survival, and engraftment of transplanted cells in the cell-sheet therapy are largely influenced by the degree of vascularization in the transplanted area and subsequent myocardial inflammation after cell-sheet transplantation.[2,17] The concept of combining OM-flap with the current cell-sheet therapy is likely to be reasonable because the OM is known to play a key role in controlling the spread of inflammation, and promoting revascularization, reconstruction and tissue regeneration. Our data suggest that the combined treatment improved the hypoxic environment in the transplanted area to a greater degree, potentially enhancing initial cell engraftment and enhancing the paracrine

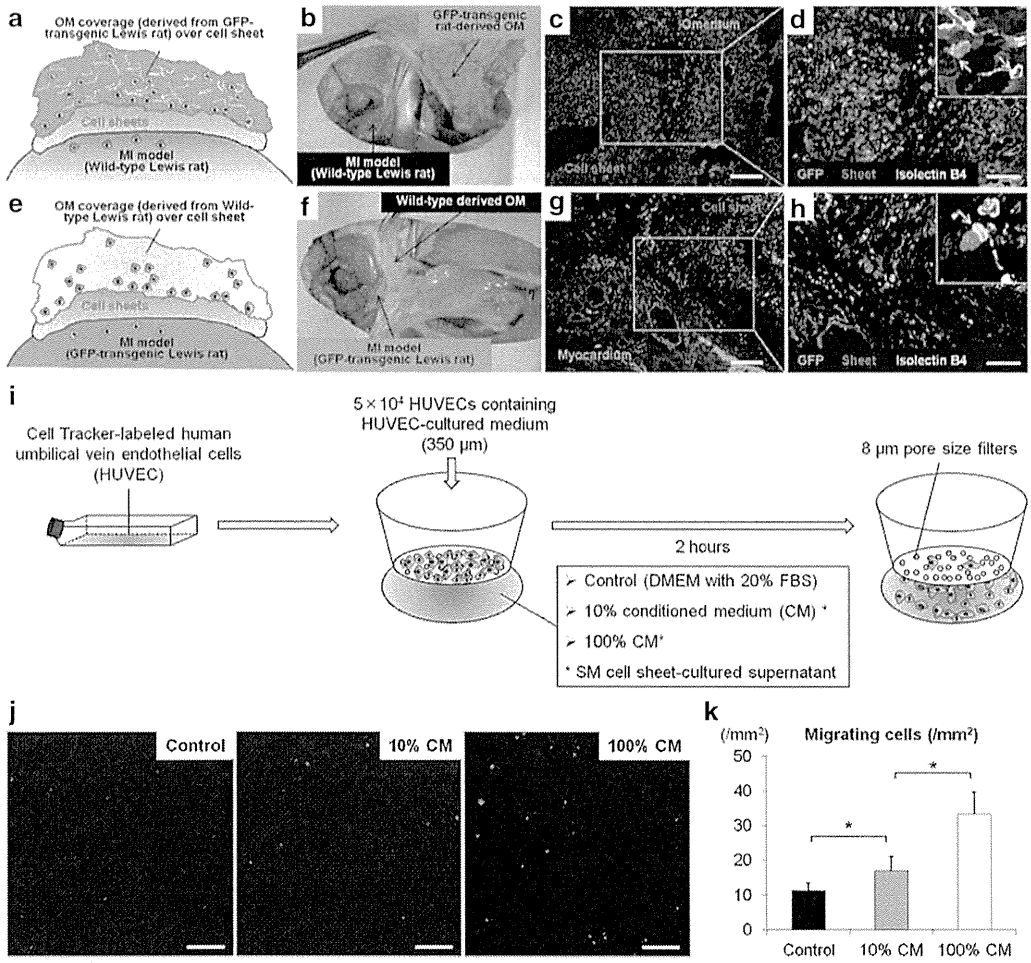


Figure 8 Schematic representation of experimental design to form parabiotic pairs of wild-type MI model rats (recipient) for transplantation of wild-type oriented cell-sheets labeled with Cell Tracker TM Orange CMTMR, followed by coverage with pedicle OM derived from GFP-transgenic rat (donor) (**a**,**b**). Representative GFP/isolectin staining in parabiotic pairs model (**c**: 100×, scale bar = 200 µm, **d**: 200×, scale bar = 100 µm). Schematic representation of experimental design to form second parabiotic pairs of GFP-transgenic MI rats for cell-sheet transplantation covered with wild-type oriented pedicle OM (**e**,**f**). Representative GFP/isolectin staining in second parabiotic pairs (**g**: 100×, scale bar = 200 µm, **h**: 200×, scale bar = 100 µm). *In vitro* migration assay (**i**). To investigate cell migration in response to skeletal myoblast cells cultured in conditioned medium, a modified Boyden chamber migration assay was performed using an HTS FluoroBlok Multiwell Insert System containing filters with a pore size of 8 µm. Human umbilical vein endothelial cells (HUVECs) were grown in EGM-2 culture medium. After incubation at 37 °C for 2 hours, the number of migrated cells was counted in 15 randomly chosen fields under 100× magnification using fluorescence microscopy. Two replicate samples were used in each experiment, which were performed at least twice. Migrating cells were analyzed using a light microscope and reported as numbers of migrating cells per mm² (**j**). Representative images show migrating cells labeled with Cell Tracker TM Orange CMTMR (100×, scale bar = 200 µm). Quantitative analyses of migrating cells according to concentration in the skeletal myoblast-cultured conditioned medium (**k**). Asterisk indicates statistical significance ($P < 0.05$).

effects induced by cell-sheet therapy in terms of higher expressions of relevant genes, potentially stabilizing therapeutic effect of cell-sheet therapy. The discrepancy between functional improvement and donor cell engraftment suggests that the improvement of cardiac function is not mainly mediated by direct contribution of transplanted donor cells but other indirect roles, possibly paracrine effects, offered by the cell-sheet at the early stage of transplantation.

The histological findings demonstrated that the rats receiving the cell-sheet implantation plus OM-flap had a significantly thickened anterior LV wall that was augmented by cardiomyocyte layers as compare to the other groups. Potential mechanisms may include cardiomyogenic differentiation of the donor-derived cells or endogenous stem cells, or paracrinal inhibition of progressive necrosis and/or apoptosis of the native cardiomyocytes. We speculate that both mechanisms might have contributed to the thickening of the targeted LV wall, although cardiomyogenic differentiation was not clearly identified in this study. Improved regional blood flow by the combined therapy could reduce the number of the necrotic/apoptotic cardiomyocytes, while reduced accumulation of fibrous components would inhibit thinning of the LV wall.[5,18] In addition, girdling effects from the covered OM might have reduced wall stress of the LV, leading to maintenance of the LV thickness.[19] Further studies to focus on the cardiomyogenic transdifferentiation using genetically labeled rodent models are warranted.

When blood vessels grow, endothelial cells migrate out first and assemble in a primitive network of immature channels

(angiogenesis).[5] As these nascent vessels only consist of endothelial cells, they rupture easily and are leaky, prone to regression, and poorly perfused.[18,20–22] Recruitment of mural cells around nascent vessels essentially contributes to remodeling and maturation of the primitive vascular network (arteriogenesis), subsequently causing therapeutic improvement of blood perfusion.[5,18] We found a larger percentage of vessels without lectin staining and lower maturation index in the control and single treatment groups, indicating that promotion of angiogenesis, but failure to effectively induce arteriogenesis. Consequently, the single treatments showed only transient effects on global cardiac function and limited functional capacity, possibly due to irregular capillary networks and increased vascular permeability. In the combined treatment group, greater numbers of functionally and structurally mature vessels were established promptly after treatment and maintained in ischemic myocardium. This might be primarily attributed to upregulated expressions of genes related to angiogenesis (*VEGF*, *VEGFR-1*, *VEGF-R2*, *Akt-1*) and/or endogenous regeneration (*SDF-1*). Moreover, elevated expressions of *Ang-1* and its receptor *Tie-2*, and *PDGF*, *VE-cadherin*, and *PECAM* might play key roles in promoting maturation processes such as "stabilization" of cell junctions and tight pericyte recruitment (arteriogenesis).[5,15,16,18,20–22] Interestingly, the elevated expression of the those relevant genes shown in the combined group was mostly reduced after 28 days after treatment (data not shown), corresponding with reduced donor cell presence. We found, however, the combined treatment group showed more sustained positive effects on vessel maturity and cardiac function recovery as compared with the control and single treatment groups at 28 days after treatment, indicating that paracrine mediators contribute to the myocardial recovery mainly during the early phase after the treatment and the effects on cardiac function and vessel structure, once established, could last for a longer time.[2] These data suggest that OM-flap covering the cell-sheet played a key role in accomplishing the maturity of the new vessels in the targeted myocardial territory, leading to formation of more organized and durable vascular network, as compared to the control and the single treatment groups.

Endothelial vasodilator function of coronary microvessels (resistance arterial vessels) is an important determinant of myocardial perfusion in response to increased myocardial oxygen demand, playing a critical role in neovascular therapies.[6–8] Vasodilation in response to specific endothelium-dependent and endothelium-independent stimuli within the coronary circulations can be measured to assess endothelial function. To the best of our knowledge, this is the first to verify that cell-sheet treatment with and without OM-flap could improve endothelial vasodilator function of resistance arterial vessels in a rat MI model, utilizing *in vivo* synchrotron-based microangiography that has proved an effective method for clearly visualizing resistance arterioles and accurately identifying neurohumoral modulation of coronary blood flow within the microcirculation for assessing therapy efficacy.[7,23,24] Microangiography revealed attenuated dilatation and a strong trend toward increased incidence of paradoxical constrictions in the control, followed by the single treatment group, suggesting that the endothelial-dependent vasodilator function in resistance arterial vessels was progressively impaired in those groups.[25,26] In contrast, combined treatment effectively restored endothelial function in resistance arterial vessels, evidenced by better dilatory responses to acetylcholine, an endothelium-dependent vasodilator.[27] This corresponds with PET/CT findings demonstrating substantial improvement in CFR, which indicated the ability of the myocardium to increase blood flow in response to increasing myocardial oxygen demand. Adenosine causes vasodilation by stimulating receptors in the microcirculation, facilitating measurement of the endothelium-independent CFR in the microcirculation. Interestingly, a remarkable improvement in CFR was observed in basal, but not apical LV, indicating that the combined treatment might be capable of improving microvasculature functionality of hibernating myocardium, rather than scar cardiac tissue. These physiological benefits in the coronary microcirculation may activate collateral growth through increased flow and shear stress, a powerful driving force of arteriogenesis, leading to enhanced functional capacity under a high load.[28,29] Therefore, we speculate that the present combined treatment strategy has potential to effectively prevent progression of endothelial dysfunction, which independently predicts major clinical adverse events in patients with heart failure.[28–30]

Our data suggest that the combination of cell sheet transplantation and OM-flap acts synergistically, rather than additively, on vessel maturation, coronary microcirculation physiology, functional capacity, and cardiac reverse remodeling, whereas the OM-only strategy failed to stabilize its long-term effect. These results encouraged us to investigate the role of the cell-sheet transplantation in activating the effects of OM-flap. Postmortem angiography findings demonstrated visible collateral vessels between the native coronary arteries and OM-flap in the combined group, whereas no tight junctions were shown in the OM-only group, indicating that formation of collateral vessels between native coronary arteries and OM was accelerated by the interposed cell-sheets. The possible mechanism of those findings might be explained by our *in vitro* migration assay demonstrating that growth factors and cytokines secreted by the cell-sheet stimulate migration of endothelial cells derived from both host myocardium and the OM toward the sheet, subsequently establishing robust vessel connections with persistent blood flow between the native coronary arteries and OM. In contrast, in the OM-only group, lack of that process caused immature leaky collateral vessel formation and thus inadequate collateral blood flow in the ischemic myocardium. Based on those findings, we speculate that the therapeutic effects of the combined treatment strategy might be responsible for increased donor cell survival and stimulation of donor cells induced by OM-flap as well as for cell-sheet–mediated activation of OM-flap as a donor artery with high perfusion capacity. Nevertheless, further studies are absolutely needed to determine the main molecular mechanism of therapeutic effects induced by the combined treatment.

## LIMITATIONS

Considering the potential molecular mechanisms behind the beneficial histological and physiological alterations observed with the combined strategy, we found that a group of possibly relevant molecules including *VEGF-A*, *VEGF receptor-1*, *VEGF receptor-2*, *Akt-1*, *SDF-1*, *PDGF-β*, *Ang-1*, *Tie-2*, *VE-cadherin*, and *PECAM* were upregulated in the combined group, suggesting that the

effects may be attributed to activation of several paracrine molecules, rather than a single molecule. Although some may argue what kinds of cytokines play a major role in generating therapeutic effects among the many complex molecular and cellular mechanisms involved, we consider that establishment of mature vessels is a complex process that is not regulated by specific factors, but rather numerous multiple factors that also dynamically change in response to the process of angiogenesis or vessel maturation. We believe that use of a cell-sheet and pedicle-OM as synergistic intelligent engineered tissues can efficiently support the regenerative process by dynamic cross-talk with ischemic cardiac tissue.

Although we did not experience any complication such as torsion of omentum flap or diaphragmatic hernia in the rats receiving the combined treatment, it is considered that a conventional lapalotomy itself may adversely affect general conditions particularly in critically-ill heart failure patients. An endoscopic approach may be useful in minimizing the OM-flap procedure-related complications in clinical settings.

## CONCLUSION

We demonstrated that cell-sheet transplantation with an omentum-flap better promoted arteriogenesis and improved coronary microcirculation physiology in ischemic myocardium tissue, leading to potent functional recovery in a rat MI model. Further development of this treatment strategy toward clinical application is encouraged.

## MATERIALS AND METHODS

All experimental procedures were approved by an institutional ethics committee. Animal care was conducted humanely in compliance with the Principles of Laboratory Animal Care formulated by the National Society for Medical Research and the Guide for the Care and Use of Laboratory Animals, prepared by the Institute of Animal Resources and published by the National Institutes of Health (publication no. 85-23, revised 1996).

Two weeks after left coronary artery ligation, rats were divided into four groups: (i) skeletal myoblast cell-sheet transplantation covered with an OM-flap (combined group), (ii) cell-sheet transplantation only, (iii) OM-flap only, and (iv) sham operation (control group). The protocol of this study is shown in Figure 1a,b. All *in vivo* and *in vitro* assessments were carried out in a blinded manner. A detailed description of all methods and reagents used for the experiments is provided in the **Supplementary Materials and Methods**.

## SUPPLEMENTARY MATERIAL

Figure S1. Frequency distribution charts showing individual segment caliber changes in response to acetylcholine in **(a)** third and **(b)** fourth branching order vessels.
Materials and Methods.

## ACKNOWLEDGMENTS

We thank Tsuyoshi Ishikawa, Yuuka Fujiwara, Yuka Kataoka, Hiromi Nishinaka, Toshika Senba, and staff of the PET Molecular Imaging Center for their excellent technical assistance. This research was supported by Research on Regenerative Medicine for Clinical Application from the Ministry of Health, Labour and Welfare of Japan and the Australian Synchrotron International Synchrotron Access Program (ISAP AS-IA111). Experiments were performed at the Japan Synchrotron Radiation Research Institute (SPring-8, BL28B2, Proposal 2011A1169). T.S. is a consultant for CellSeed, Inc., and T.O. is an Advisory Board Member of CellSeed, Inc. and an inventor/developer holding a patent for temperature-responsive culture surfaces. The authors have no conflicts of interest to report.

## REFERENCES

1. Shah, AM and Mann, DL (2011). In search of new therapeutic targets and strategies for heart failure: recent advances in basic science. *Lancet* **378**: 704–712.
2. Narita, T, Shintani, Y, Ikebe, C, Kaneko, M, Harada, N, Tshuma, N *et al.* (2013). The use of cell-sheet technique eliminates arrhythmogenicity of skeletal myoblast-based therapy to the heart with enhanced therapeutic effects. *Int J Cardiol* **168**: 261–269.
3. Sekiya, N, Matsumiya, G, Miyagawa, S, Saito, A, Shimizu, T, Okano, T *et al.* (2009). Layered implantation of myoblast sheets attenuates adverse cardiac remodeling of the infarcted heart. *J Thorac Cardiovasc Surg* **138**: 985–993.
4. Habib, GB, Heibig, J, Forman, SA, Brown, BG, Roberts, R, Terrin, ML *et al.* (1991). Influence of coronary collateral vessels on myocardial infarct size in humans. Results of phase I thrombolysis in myocardial infarction (TIMI) trial. The TIMI Investigators. *Circulation* **83**: 739–746.
5. Carmeliet, P and Jain, RK (2011). Molecular mechanisms and clinical applications of angiogenesis. *Nature* **473**: 298–307.
6. Gutiérrez, E, Flammer, AJ, Lerman, LO, Elízaga, J, Lerman, A and Fernández-Avilés, F (2013). Endothelial dysfunction over the course of coronary artery disease. *Eur Heart J* **34**: 3175–3181.
7. Shirai, M, Schwenke, DO, Tsuchimochi, H, Umetani, K, Yagi, N and Pearson, JT (2013). Synchrotron radiation imaging for advancing our understanding of cardiovascular function. *Circ Res* **112**: 209–221.
8. Furchgott, RF and Zawadzki, JV (1980). The obligatory role of endothelial cells in the relaxation of arterial smooth muscle by acetylcholine. *Nature* **288**: 373–376.
9. Banquet, S, Gomez, E, Nicol, L, Edwards-Lévy, F, Henry, JP, Cao, R *et al.* (2011). Arteriogenic therapy by intramyocardial sustained delivery of a novel growth factor combination prevents chronic heart failure. *Circulation* **124**: 1059–1069.
10. O'Shaugnessy, L (1937). Surgical treatment of cardiac ischemia. *Lancet* **232**: 185–194.
11. Takaba, K, Jiang, C, Nemoto, S, Saji, Y, Ikeda, T, Urayama, S *et al.* (2006). A combination of omental flap and growth factor therapy induces arteriogenesis and increases myocardial perfusion in chronic myocardial ischemia: evolving concept of biologic coronary artery bypass grafting. *J Thorac Cardiovasc Surg* **132**: 891–899.
12. Shrager, JB, Wain, JC, Wright, CD, Donahue, DM, Vlahakes, GJ, Moncure, AC *et al.* (2003). Omentum is highly effective in the management of complex cardiothoracic surgical problems. *J Thorac Cardiovasc Surg* **125**: 526–532.
13. Shudo, Y, Miyagawa, S, Fukushima, S, Saito, A, Shimizu, T, Okano, T *et al.* (2011). Novel regenerative therapy using cell-sheet covered with omentum flap delivers a huge number of cells in a porcine myocardial infarction model. *J Thorac Cardiovasc Surg* **142**: 1188–1196.
14. Kawamura, M, Miyagawa, S, Fukushima, S, Saito, A, Miki, K, Ito, E *et al.* (2013). Enhanced survival of transplanted human induced pluripotent stem cell-derived cardiomyocytes by the combination of cell sheets with the pedicled omental flap technique in a porcine heart. *Circulation* **128**(11 Suppl 1): S87–S94.
15. Mancuso, MR, Davis, R, Norberg, SM, O'Brien, S, Sennino, B, Nakahara, T *et al.* (2006). Rapid vascular regrowth in tumors after reversal of VEGF inhibition. *J Clin Invest* **116**: 2610–2621.
16. Inai, T, Mancuso, M, Hashizume, H, Baffert, F, Haskell, A, Baluk, P *et al.* (2004). Inhibition of vascular endothelial growth factor (VEGF) signaling in cancer causes loss of endothelial fenestrations, regression of tumor vessels, and appearance of basement membrane ghosts. *Am J Pathol* **165**: 35–52.
17. Shimizu, T, Sekine, H, Yang, J, Isoi, Y, Yamato, M, Kikuchi, A *et al.* (2006). Polysurgery of cell sheet grafts overcomes diffusion limits to produce thick, vascularized myocardial tissues. *FASEB J* **20**: 708–710.
18. Carmeliet, P and Conway, EM (2001). Growing better blood vessels. *Nat Biotechnol* **19**: 1019–1020.
19. Hagège, AA, Vilquin, JT, Bruneval, P and Menasché, P (2001). Regeneration of the myocardium: a new role in the treatment of ischemic heart disease? *Hypertension* **38**: 1413–1415.
20. Weis, SM and Cheresh, DA (2005). Pathophysiological consequences of VEGF-induced vascular permeability. *Nature* **437**: 497–504.
21. Cao, Y, Hong, A, Schulten, H and Post, MJ (2005). Update on therapeutic neovascularization. *Cardiovasc Res* **65**: 639–648.
22. Adams, RH and Alitalo, K (2007). Molecular regulation of angiogenesis and lymphangiogenesis. *Nat Rev Mol Cell Biol* **8**: 464–478.
23. Jenkins, MJ, Edgley, AJ, Sonobe, T, Umetani, K, Schwenke, DO, Fujii, Y *et al.* (2012). Dynamic synchrotron imaging of diabetic rat coronary microcirculation in vivo. *Arterioscler Thromb Vasc Biol* **32**: 370–377.
24. Iwasaki, H, Fukushima, K, Kawamoto, A, Umetani, K, Oyamada, A, Hayashi, S *et al.* (2007). Synchrotron radiation coronary microangiography for morphometric and physiological evaluation of myocardial neovascularization induced by endothelial progenitor cell transplantation. *Arterioscler Thromb Vasc Biol* **27**: 1326–1333.
25. Ludmer, PL, Selwyn, AP, Shook, TL, Wayne, RR, Mudge, GH, Alexander, RW *et al.* (1986). Paradoxical vasoconstriction induced by acetylcholine in atherosclerotic coronary arteries. *N Engl J Med* **315**: 1046–1051.
26. Marti, CN, Gheorghiade, M, Kalogeropoulos, AP, Georgiopoulou, VV, Quyyumi, AA and Butler, J (2012). Endothelial dysfunction, arterial stiffness, and heart failure. *J Am Coll Cardiol* **60**: 1455–1469.
27. Bonetti, PO, Lerman, LO and Lerman, A (2003). Endothelial dysfunction: a marker of atherosclerotic risk. *Arterioscler Thromb Vasc Biol* **23**: 168–175.
28. Poelzl, G, Frick, M, Huegel, H, Lackner, B, Alber, HF, Mair, J *et al.* (2005). Chronic heart failure is associated with vascular remodeling of the brachial artery. *Eur J Heart Fail* **7**: 43–48.
29. Meyer, B, Mörtl, D, Strecker, K, Hülsmann, M, Kulemann, V, Neunteufl, T *et al.* (2005). Flow-mediated vasodilation predicts outcome in patients with chronic heart failure: comparison with B-type natriuretic peptide. *J Am Coll Cardiol* **46**: 1011–1018.
30. Heitzer, T, Baldus, S, von Kodolitsch, Y, Rudolph, V and Meinertz, T (2005). Systemic endothelial dysfunction as an early predictor of adverse outcome in heart failure. *Arterioscler Thromb Vasc Biol* **25**: 1174–1179.

**Figure S1**

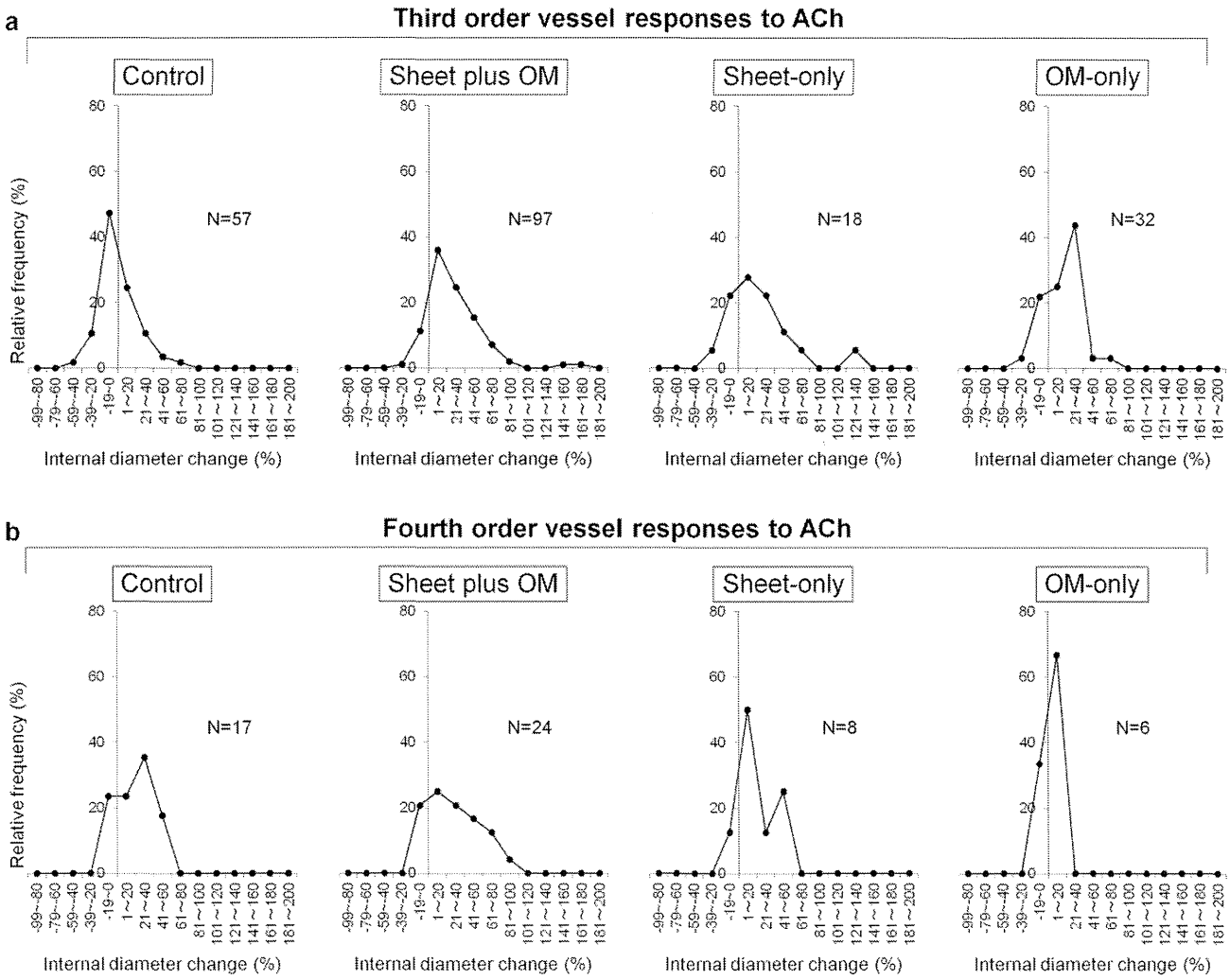
a
Third order vessel responses to ACh
Control
Sheet plus OM
Sheet-only
OM-only
N=57
N=97
N=18
N=32
Relative frequency (%)
Internal diameter change (%)
b
Fourth order vessel responses to ACh
Control
Sheet plus OM
Sheet-only
OM-only
N=17
N=24
N=8
N=6
Relative frequency (%)
Internal diameter change (%)

## Supplemental figure legends

### Figure S1

Frequency distribution charts showing individual segment caliber changes in response to acetylcholine in **(a)** third and **(b)** fourth branching order vessels. The control group had a relatively high frequency of third and fourth branching order arterial vessels showing localized segmental vasoconstriction (ID constriction >5% of baseline). The frequency of abnormal vasoconstriction with acetylcholine in the control group was about 8- and 4-fold for the third and fourth branching order, respectively, as compared with the combined group (third order: control 49% vs. combined 6% vs. sheet-only 22% vs. OM-only 25%; fourth order: control 18% vs. combined 4% vs. sheet-only 13% vs. OM-only 17%).

## Supplemental Materials and Methods

### *Construction of Cell-sheets*

Skeletal myoblasts were isolated from tibialis anterior muscle tissues of 3-week-old male wild-type or GFP transgenic Lewis rats as appropriate, and cultured as previously described.[1] In brief, when the cells became approximately 70% confluent after 4 days of cultivation in Dulbecco's modified Eagle Medium (DMEM) (Gibco) with 20% fetal bovine serum (Sigma-Aldrich), they were transferred to 35-mm temperature-responsive culture dishes (UpCell, Cellseed, Tokyo, Japan) and incubated at 37°C, with the cell number adjusted to $3.0\times10^6$ per dish. After 24 hours, the cells were induced to spontaneously detach by cooling at 20°C for 30 minutes, which yielded a scaffold-free sheet-shaped monolayer of skeletal myoblasts for use as a graft.

### *Establishment of Chronic Myocardial Infarction Rat Model*

Two hundred female Lewis rats (180-200 g, Charles River) underwent left coronary artery ligation as previously described.[1] The rats were anaesthetized by inhalation of isoflurane (2%, 0.2 mL/min), intubated, and placed on a respirator during surgery to maintain ventilation. The carrier gas for isoflurane is oxygen. The adequacy of anaesthesia was monitored by electrocardiography and pulse rate. Two weeks after left coronary artery ligation, transthoracic echocardiography was performed to validate the extent of myocardial infarction (MI). We aimed to create a widespread MI model, thus rats with a small extent of wall motion abnormality with ejection fraction greater than 45% were excluded **(Figure 1)**. The widespread chronic MI models were randomly divided into 4 treatment groups: 1) cell-sheet transplantation covered with omentum (OM)-flap (combined group), 2) cell-sheet transplantation (sheet-only group), 3) OM-flap (OM-only group), and 4) sham operation

(control group) **(Figure 1)**. In the sheet-only group, a five-layered cell-sheet was placed on the area and spread manually to cover both infarct and border areas. In the OM-only group, a small upper midline laparotomy was performed to manipulate the OM tissue. After making a small hole in the diaphragm, the pedicle OM-flap was then pulled from the peritoneal space to the pleural cavity using a transdiaphragmatic approach and wrapped directly onto the epicardium in the ischemic area. In the combined group, 5-layered cell-sheets were placed in a similar manner as in the sheet-only group, then covered with the harvested OM-flap.

***Histological Analysis***

Four weeks after the treatment, the rats were humanely killed by an intraperitoneal injection of pentobarbital (300 mg/kg) and heparin (150 U) for histological analysis of the heart tissue (n=11 for each group) **(Figure 1)**. Anterior wall thickness was measured in at least 3 hematoxylin and eosin-stained sections of the middle portion of the LV, while Sirius red staining was performed to assess myocardial fibrosis in the peri-infarct region. The fibrotic region was calculated as the percentage of myocardial area. Data were obtained from 5 individual views of each heart. Periodic acid-Schiff staining was performed to examine the degree of cardiomyocyte hypertrophy. Myocyte size was determined by drawing point-to-point perpendicular lines across the cross-sectional area of the cell at the level of the nucleus. The results are expressed as the average diameter of 20 myocytes randomly selected from 5 fields of each ventricle. The images were examined by optical microscopy (Olympus, Tokyo, Japan) and quantitative morphometric analysis for each sample was performed using Metamorph software (Molecular Devices, Sunnyvale, California, US).

***RNA Extraction and Quantitative Reverse-transcription Polymerase Chain Reaction***

The myocardial gene expressions related to angiogenesis, vessel maturation, and anti-inflammation at 3 days after the treatment were assessed by quantitative reverse transcription PCR **(Figure 2)**. Total RNA was extracted from the peri-infarct myocardium using an RNeasy mini kit (Qiagen GmbH, Hilden, Germany), according to the manufacturer's instructions. For each sample, 1 μg of total RNA was converted to cDNA with Omniscript RT (Qiagen) and analyzed with a PCR array (Qiagen-SABiosciences) and Applied Biosystems® ViiA™ 7 real-time PCR system (Life Technologies Corporation). Data were normalized to β-actin expression level. Relative gene expression was determined using the ΔΔCT method.

***Immunohistochemistry***

Endothelial cells were labeled with rat monoclonal anti-CD31 antibody (Abcam, Cambridge, UK 1:50), while pericytes were labeled with mouse monoclonal anti-α-SMA antibody (DAKO, Glostrup, Danmark 1:50) and visualized by corresponding secondary antibodies (Alexafluor 488 or Alexafluor555; Alexafluor 647 Molecular Probes, Eugene, OR), then counterstained with Hoechst 33342 (Dojindo, Kumamoto, Japan). Vessel density and maturity were quantified as the number of CD31 positive vessels and CD31/α-SMA double-positive vessels per $mm^2$, respectively. A maturation index was calculated as the percentage of CD31/α-SMA double-positive vessels to total vessel number. Vessels positive for CD31 but negative for lectin were regarded as functionally immature vessels undergoing regression or that had lost patency.[2]

***Evaluation of Mature Vessels with Patent Endothelial Layers***

Mature vessels with patent endothelial layers were assessed by injection of 500 μl of Alexa Fluor 568 conjugate-labeled esculentum lectin (500 μg in 500 uL in 0.9% NaCl; GS-IB4,

Molecular Probes, Eugene, OR), which binds uniformly and rapidly to the luminal surface of endothelium and thus labels patent blood vessels, into a tail vein 30 minutes before tissue sampling.[2] Myocardial tissues were then removed, immersed in fixative for 1 hour in 4% paraformaldehyde, rinsed several times with PBS, infiltrated with 30% sucrose, frozen in OCT compound, and processed for immunohistochemistry.

***Vessel Recruitment in the Transplanted Cell-sheets***

To evaluate the angiogenic effect of the OM-flap in the transplanted area, we serially assessed the number of functional blood vessels with patent endothelial layers (CD31/lectin double-positive cells) in the transplanted area of the sheet-only and combined groups at 3, 7 and 28 days after each treatment (n=6 for each group and each time point) **(Figure 3)**.

***Vessel Remodeling and Maturation in Peri-infarct Myocardium***

We serially assessed neovascular vessel maturity in peri-infarct areas at 3 (n=6 for each group) and 28 days (n=11 for each group) after treatment **(Figure 4)**. Vessel density and structural maturity were quantified as the number of CD31 positive and CD31/α-smooth muscle actin (SMA) double-positive vessels per $mm^2$, respectively. A maturation index was calculated as the percentage of CD31/α-SMA double-positive vessels to total vessel number.

***Synchrotron radiation microangiography***

To evaluate the effects of each treatment on microcirculation physiology in terms of relative dilatory responses to acetylcholine and dobutamine hydrochloride in the resistance vessels, synchrotron radiation microangiography was performed after 3 weeks after the treatment (control: n=11, combined: n=11, cell-sheet: n=5, OM: n=6) at SPring-8, Japan Synchrotron